Supporting Information:

Characterization of Kerogen and Source Rock Maturation Using Solid-State NMR Spectroscopy

Andrew Clough, Jessica L. Sigle, David Jacobi,[±] Jeff Sheremata,[±]
and Jeffery L. White*
Department of Chemistry, Oklahoma State University, Stillwater, OK 74078

Interrupted Decoupling

Testing for optimal decoupling delays was performed using a ^{13}C RACP-MAS at 10 kHz (rotor period = 100 μs) with a rotor synchronized spin echo (τ-180°-τ) before acquisition. The ^{1}H decoupling is turned on after the contact pulse and a delay that can vary between 0 μs and the rotor period (i.e. decoupling always starts before the spin echo pulse), and remains on until data acquisition is finished. Testing was first performed using glycine, which has both a protonated and non-protonated carbon with narrow, distinct ^{13}C resonances. Figure S1a shows that with this rotor synchronized method, the non-protonated glycine signal remains unchanged as the ^{1}H decoupling delay is varied between 0 μs and 100 μs, while the protonated signal disappears for delays ≥ 40 μs. The increase in the protonated signal at 100 μs is likely the result of the decoupling being delayed by one full rotor period and starting right at the beginning of the spin echo pulse. Based on this data, a decoupling delay of 50 μs should be sufficient to distinguish protonated from non-protonated aromatic carbons in the kerogen. To verify that this is indeed the case, interrupted decoupling experiments with delay times up to 50 μs were performed on Ker-E using RACP-MAS at 10 kHz. Figure S1b shows the integrated peak intensity for total contact times of 200 μs (filled symbols) and 1 ms (open symbols). The aliphatic and aromatic intensities reach a plateau by 40 μs. The behavior of the aromatic intensity is consistent with the results from glycine, as the plateau indicates that the contribution of protonated aromatic carbons

to the signal intensity vanishes by 40 μs. For the aliphatic peak, the intensity remaining in the plateau comes from molecular groups that undergo fast motions, such as methyl groups and methylene directly attached to the methyl groups. While the aliphatic intensity follows a similar trend for both the 200 μs and 1 ms contact times, with ~ 29 % of the original signal intensity remaining in the plateau, more signal remains in the aromatic peak with the longer contact time of 1 ms (53 %) than with 200 μs (33 %). This increase in the non-protonated fraction of aromatic carbons is consistent with a long T_{CH} for the non-protonated aromatic carbons.

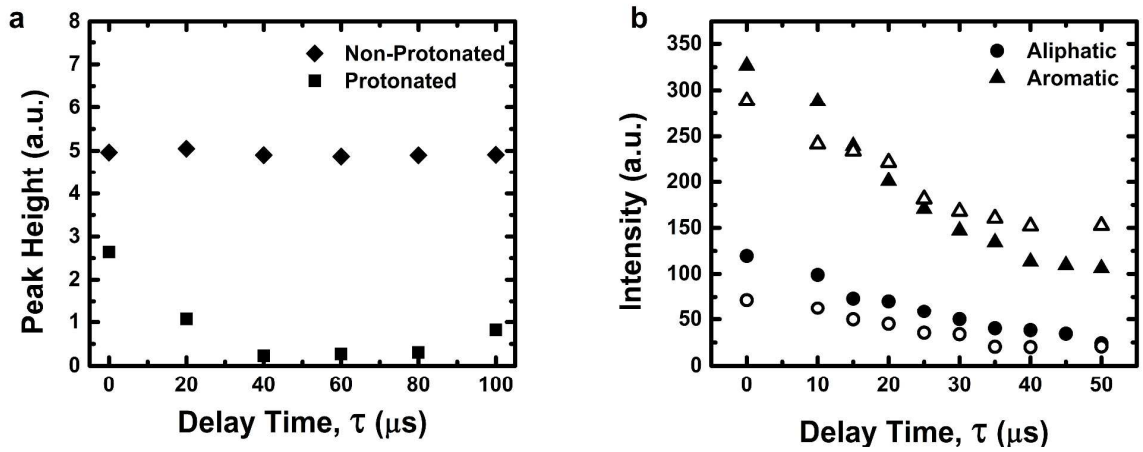

Figure S1. Results from 10 kHz ^{13}C RACP-MAS with rotor synchronized interrupted decoupling for a) glycine and b) Ker-E. In glycine, the non-protonated signal (♦) remains constant, while the protonated signal (■) is fully removed once the ^{1}H decoupling delay (τ) is ≥ 40 μs. For the kerogen sample using a 200 μs contact time (filled symbols) and 1 ms contact time (open symbols), both the aliphatic (●) and aromatic (▲) integrated intensities reach a plateau by τ = 40 μs.

As differences are observed between the results of interrupted decoupling using DP-MAS and RACP-MAS for both the surviving aromatic and aliphatic intensities, and most ssNMR studies on kerogen have relied on CP-MAS, additional tests were performed on four kerogen samples using CP-MAS based interrupted decoupling at 5 kHz (200 μs rotor period) with contact times of 500 μs, 1 ms, and 1.5 ms, the results of which are given in Table S1 along with the 10

kHz DP-MAS results. The values of f_{NP}^{Ar} are seen to increase with increasing contact time for all samples, suggesting that at longer contact times, f_{NP}^{Ar} may reach the value obtained using DP-MAS, though with a considerable loss in signal intensity due to the short $T_{1\rho}^{H}$ observed. The f_{fast}^{Al} measured with CP-MAS in each sample is also significantly lower than that observed using DP-MAS, but there is no systematic change as the contact time is increased. The f_{fast}^{Al} values are similar to the value observed for Ker-E with RACP-MAS. This is likely the result of rigid spins being emphasized over more mobile spins with cross-polarization, while the aliphatic signal remaining after the 50 µs interrupted decoupling delay are the aliphatic chain ends, which are not as rigid as the rest of the aliphatic components.

Table S1. Fraction of aromatic carbons that are non-protonated (f_{NP}^{Ar}) and aliphatic carbons that have fast-motion aliphatic carbon (f_{fast}^{Al}) as determined by interrupted decoupling using DP-MAS at 10 kHz and CP-MAS at 5 kHz with contact times of 500 µs, 1 ms, and 1.5 ms.

Sample	**DP-MAS 10 kHz**		**CP-MAS 500 µs**		**CP-MAS 1 ms**		**CP-MAS 1.5 ms**	
	f_{NP}^{Ar}	f_{fast}^{Al}	f_{NP}^{Ar}	f_{fast}^{Al}	f_{NP}^{Ar}	f_{fast}^{Al}	f_{NP}^{Ar}	f_{fast}^{Al}
Ker-A	0.73	0.57	0.52	0.22	0.54	0.28	0.62	0.26
Ker-B	0.77	0.48	0.44	0.14	0.48	0.23	0.68	0.32
Ker-C	0.76	0.49	0.38	0.15	0.56	0.21	0.60	0.18
Ker-E	0.79	0.63	0.43	0.24	0.52	0.23	0.63	0.17

Spin-counting

Spin-counting measurements were performed on 73.6 mg of sample Rock-B confined to the center (ca. 20 % of total rotor volume) of a 7 mm diameter rotor using boron nitride spacers. The choice of boron nitride for the spacer material was made in order to acquire both ^{1}H and ^{13}C DP-MAS spectra, as other materials typically used for rotor spacers, such as Teflon, have carbon

signals observable when performing ^{13}C DP-MAS. A small amount (0.68 mg) of polydimethylsiloxane (PDMS) was added to the sample as an internal standard. This PDMS mass was chosen in order for the ^{13}C PDMS signal to be well resolved above the background and for the ^{1}H PDMS peak to not be too large relative to the sample signal.

A quantitative ^{13}C DP-MAS spectrum was acquired with a 5 μs 90° pulse width, repetition delay of 15 s, and 8K transients using the modified EASY background suppression technique described in the experimental section. Figure S2a shows the ^{13}C spectra after subtraction of the background acquired from the second acquisition of the EASY technique, the additional background as measured with an empty rotor, and the resulting sample signal. The narrow PDMS peak occurs near 2 ppm, well resolved from the sample signal, allowing for the total intensity of the PDMS and the organic content of the rock to be measured. While the signal to noise ratio of the sample is poor, an overlay with the ^{13}C DP-MAS spectrum of ca. 500 mg of Rock-B completely filling the rotor shows good agreement between the two different amounts of sample, as shown in Figure S2b. This indicates that the background removal procedure employed here is very effective, as any background not accounted for would be more prominent in the spin-counting spectrum and distort the spectrum's shape away from that of the full rotor spectrum. The PDMS integrated intensity is used to determine the intensity per carbon. Since all ^{13}C signals are within the homogenous field region of the coil, the intensity of the organic content of the rock can be converted into a total number of carbon atoms, from which the total carbon mass can be compared to the total sample mass to obtain the organic carbon wt. %, which is found to be 1.85 %.

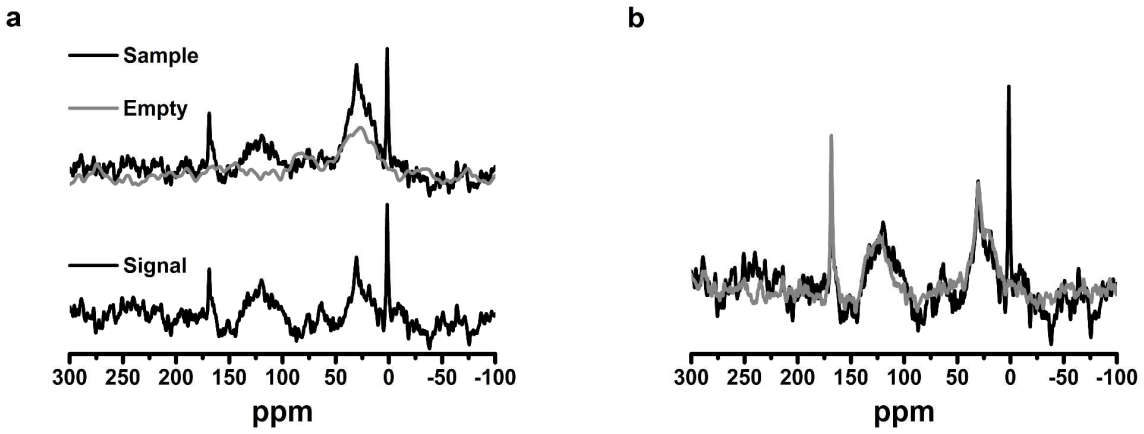

Figure S2. 5 kHz ^{13}C DP-MAS spectra of a) Rock-B with an internal PDMS spin-counting standard, both after removal of background using the EASY background suppression method and after removal of background not picked up by the second acquisition of the EASY sequence as determined from an empty rotor, and b) a comparison of the spectra from spin-counting (black) and from a full rotor (gray) normalized to the same scale.

Additionally, ^{1}H spin-counting measurements can be made. Both static and 5 kHz MAS ^{1}H spectra were acquired using a single 5 μs 90° pulse width, a repetition delay of 10 s (in order to allow for full spin-lattice relaxation of the PDMS), and 128 transients. In the static spectrum, there is significant overlap between the PDMS peak (chemical shift ca. 0.4 ppm) and the mobile component of the rock sample. A simple method for resolving the PDMS peak from the sample signal is to overlay this spectrum with that of the corresponding spectrum of the sample occupying the full rotor, normalizing the two such that the portions of the spectra away from the PDMS signal region match, and subtracting the two spectra in order to obtain a spectrum only containing the PDMS signal. A similar method to that described for carbon is used to find the intensity per ^{1}H from the PDMS signal and then find the number of ^{1}H in the sample. An additional step of converting from number of hydrogen atoms to carbon atoms is performed using the H:C ratio found experimentally for the rock sample (4.38). Using this method, the organic carbon wt. % is found to be 2.3 %. The same measurement can be performed with the 5

kHz MAS spectrum shown in Figure S3. As can be seen by the inset, the PDMS peak can easily be distinguished from the signal coming from the rock. Using the same method as described for the static case, the organic carbon wt. % is found to be 2.4 %, which is consistent with the value measured from the static spectrum. Thus, ^{13}C DP-MAS gives an organic carbon wt. % of 1.85 %, while ^{1}H spin-counting gives a value of 2.35 %. While not exactly the same, these two different methods give consistent results, particularly given the low signal to noise ratio associated with the ^{13}C DP-MAS spectrum of the sample. Taking the average of these two methods (2.1 %) as the measured organic carbon wt. %, we note that the individual ^{13}C or ^{1}H measurements differ by 12 % of the average value, which provides an estimate of the uncertainty in this measurement.

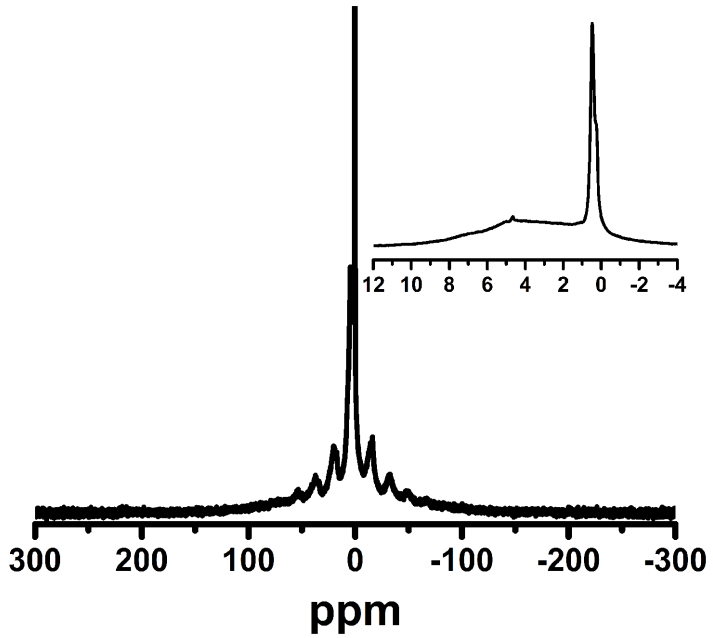

Figure S3. 5 kHz ^{1}H spin-counting spectrum of Rock-B. The inset shows the isotropic region, clearly showing that the PDMS peak at 0.4 ppm is easily distinguished from the mobile component of the rock sample.